The 2010 IEEE/RSJ International Conference on
Intelligent Robots and Systems
October 18-22, 2010, Taipei, Taiwan

# Antagonistically Actuated Compliant Joint: Torque and Stiffness Control

I. Sardellitti[1], G. Palli[2], N. G. Tsagarakis [1] and D. G. Caldwell[1]

*Abstract*— **The current research effort in the design of lightweight and safe robots is resulting in increased interest for the development of variable stiffness actuators. Antagonistic pneumatic muscle actuators (pMAs) have been proposed for this purpose, due to their inherent nonlinear spring behavior resulting from both air compressibility and their nonlinear force-length relation. This paper addresses the simultaneous torque and stiffness control of an antagonistically actuated joint with pneumatic muscles driven by compact, fast-switching solenoid valves. This strategy allows compensation of unmodeled joint dynamics while adjusting the joint stiffness depending on the task requirements. The proposed controller is based on a sliding mode force control applied to an average model of the valve-pneumatic muscle system. This was necessary to cope with both the well known model uncertainties of the pMA and the discontinuous on-off behavior of the solenoid valves. Preliminary experimental results verified the effectiveness of the proposed implementation.**

## I. Introduction

One of the current challenges in robotics is the introduction of robots in the human environment and, as a consequence, the improvement of safety in human-robot interaction. This increasing vicinity between humans and robots requires a significant innovation in the traditional robot design, both in the hardware and in the software level. As a result, considerable research effort has been devoted to decrease the risks of collisions between humans and robots, enhancing the awareness of the robot about the surrounding environment through sensors and sophisticated control strategies [1]. Moreover, increasing attention has been placed on reducing the impact forces in the case of an unexpected collision, through the development of new robots with lightweight structures [2], and new actuation strategies [3].

Variable stiffness actuators have been proposed as a safe approach for driving robots that interact with humans [4]. These actuators allow a robot to both absorb the energy of an impact through a compliant mechanism, and to achieve precise joint positioning through variation of the stiffness. Several mechanical arrangements have been explored to develop variable stiffness actuators, e.g. the antagonistic approach, with a pair of actuators coupled through nonlinear springs in series [5], [6], or two independent actuators, one for the joint positioning and one for the adjustment of the stiffness [7]. Within the antagonistic configurations, the use of pneumatic muscles has also been proposed in [8], [9], since this technology naturally behaves like a nonlinear spring, without the need of extra components.

However the widespread use of the pneumatic muscle actuation has been hampered by the difficulties in achieving a precise position or force control. This is mainly due to phenomena such as viscous friction [10], hysteresis [11] and the variation of muscle characteristics due to fatigue [12], which are difficult to model. In addition, pneumatic muscles used in robotics applications are mostly driven by solenoid valves because of their low cost, reduced size, and weight. However, the discontinuous on/off nature of the solenoid valves further reduces the accuracy of the system, making it difficult to achieve smooth control.

Several control strategies have been proposed for antagonistic pneumatic muscles to achieve simultaneous joint position and stiffness control through adjustment of the pneumatic muscle's inner pressure. In [13] and [14] the performance of adaptive and PID control strategies were explored; the pneumatic valve characteristics, however, were not considered in the design of the controller. In [15] a PID control strategy combined with feedback linearization was proposed. In this case the valve model was considered and a bang bang control was implemented for adjusting the pressure in the muscles.

Although such approaches guaranteed an effective control of the joint, this paper proposes a simultaneous torque and stiffness controller. The advantage of building a torque control loop rather then position consists in the possibility of directly compensating for the mechanical system dynamics (in case the joint is used to drive a kinematic chain, e.g. a robotic arm) and external loads, allowing the decoupled control of the motion in systems with several DOFs. The joint controller takes advantage of the antagonistic actuation mathematical model as well as the nonlinear spring behavior of the pneumatic muscles as described in [11], to determine the forces necessary at each muscle for tracking the required joint torque and stiffness profiles. A sliding mode force controller is then implemented on each muscle, since it is a well known robust strategy able to tackle the parametric and modeling uncertainties of a system such as the pMA [16]. The control signal is finally converted into a duty cycle for the PWM driven solenoid valves in order to achieve a smoother control of the valve flow rate and therefore of the pneumatic actuators [17], [18].

[1] I. Sardellitti, N. G. Tsagarakis, D. G. Caldwell are with the Advanced Robotics Lab., Italian Institute of Technology, Genoa, Italy. email: {irene.sardellitti, nikos.tsagarakis, darwin.caldwell}@iit.it

[2] G. Palli is with the Department of Electronics, Computer Science and Systems, University of Bologna, Italy. email: gianluca.palli@unibo.it

This paper is structured as follows. In Sec. II the mathematical model of the valve-pneumatic muscle system is discussed. Sec. III describes the simultaneous torque and stiffness control for one joint driven by antagonistic pMAs, while Sec. IV reports on the experimental results. The paper concludes with a summary of the work.

## II. Model Of The Pneumatic System

Most of models of pMA presented in literature establish a relation between the force provided by the muscle and the inner pressure of the muscle itself, as a function of some characteristic parameters of the braided structure [11]. A classic formulation of this relation is

$$F = \frac{P}{4\pi n^2}(3L^2 - b^2) \tag{1}$$

where $P$ is the relative pressure in the pneumatic muscle, approximated as perfect cylinder with length $L = b\cos(\theta)$. The braided layer wrapped around the muscle is modeled with strands of length $b$, that surround in a helical manner $n$ times the cylinder at angle $\theta$ with respect to the main axis of the cylinder. It is clear from (1) that the pneumatic muscles do not generate force ($F = 0$) either for null inner relative pressure ($P = 0$), or for maximal shortening, reached when $\theta = 54.7°$ for the muscles considered in this paper. In addition, from (1), it is also noticeable that the change in force exerted by the pMA also depends on the change of length. This, combined with the air compressibility, gives to the pMA the well known spring like behavior. In more detail, a formulation of the stiffness $k$ is obtained through the derivation of the force in (1) with respect to its length as

$$k = \frac{dP}{dL}\left(\frac{3L^2 - b^2}{4\pi n^2}\right) + \frac{3PL}{2\pi n^2}. \tag{2}$$

Assuming small volume and pressure variations with respect to the length around the working point, the term $\frac{dP}{dL}$ can be neglected [19]. As a result, the stiffness of the pMA is simplified as

$$k = \frac{3PL}{2\pi n^2} \tag{3}$$

and it depends on the actual muscle's pressure and length. In this application the pneumatic muscle is driven by two solenoid valves, for pressurizing and depressurizing respectively. A simplified model of the muscle pressure variations $\dot{P}$ during the three different working phases of the valves has been implemented. This model considers the overall valve-pneumatic muscle system as a first-order dynamic model. This simplification is extensively used in literature by [20], [21] and it relies on the assumption that the pneumatic muscle volume variation is small around the working point, and the dynamics of the valve are much faster than those of the muscles, therefore it can be neglected. Given this assumption, the pressure variation in the pneumatic muscle can be described as:

$$\dot{P} = \begin{cases} -\frac{P}{\tau} + \frac{Ps}{\tau} & \text{when } d_1 = 1,\ d_2 = 0 \\ 0 & \text{when } d_1 = 0,\ d_2 = 0 \\ -\frac{P}{\tau} & \text{when } d_1 = 0,\ d_2 = 1 \end{cases} \tag{4}$$

where $\tau$ is the time constant of the valve-muscle system, $P_s$ is the pressure supply and $d_1$, $d_2$ are the input command signals of the pressurizing and depressurizing valves, respectively. Given the on-off behavior of the solenoid valves the command signals $d_1$, $d_2$ take values in the discrete set $\{0, 1\}$; note also that the two valves cannot work simultaneously, therefore the case $d_1 = 1$, $d_2 = 1$ is not considered.

## III. Torque and stiffness control

Pneumatic muscle actuation on its own can only generate pulling forces, therefore a pair of actuators were coupled through a pulley to generate bidirectional torques (Fig. 3). A simultaneous stiffness and torque controller was then implemented on the antagonistically actuated 1 DOF joint through pneumatic muscle force control. This was obtained by considering

$$T_J = r(F_1 - F_2) \tag{5}$$

$$S_J = r^2(k_1 + k_2) \tag{6}$$

where $T_J$ is the joint torque, $S_J$ is the joint stiffness, $r$ is the radius of the pulley, $F_i$ and $k_i$ are the force and stiffness at each muscle $i \in \{1, 2\}$ according to eq. (1) and (3) respectively.

Given the desired joint torque and stiffness profiles $T_d$ and $S_d$, from eq. (1), (3), (5) and (6) the desired pressure profiles $P_{id}$ of the two antagonistic muscles can be defined as

$$P_{1d}\,(3L_1^2 - b^2) - P_{2d}\,(3L_2^2 - b^2) = \frac{4\,\pi\,n^2}{r}\,T_d \tag{7}$$

$$P_{1d}\,L_1 + P_{2d}\,L_2 = \frac{2\,\pi\,n^2}{3\,r^2}\,S_d \tag{8}$$

where $L_i$ are the actual lengths of the pneumatic muscles. By rearranging (7) and (8) as

$$Q \begin{bmatrix} P_{1d} \\ P_{2d} \end{bmatrix} = \begin{bmatrix} \frac{4\,\pi\,n^2}{r}\,T_d \\ \frac{2\,\pi\,n^2}{3\,r^2}\,S_d \end{bmatrix} \tag{9}$$

where

$$Q = \begin{bmatrix} 3L_1^2 - b^2 & -(3L_2^2 - b^2) \\ L_1 & L_2 \end{bmatrix}. \tag{10}$$

the desired force profiles $F_{id}$ are obtained through (9), (1) and (3)

$$\begin{bmatrix} F_{1d} \\ F_{2d} \end{bmatrix} = \begin{bmatrix} 3L_1^2 - b^2 & 0 \\ 0 & 3L_2^2 - b^2 \end{bmatrix} Q^{-1} \begin{bmatrix} \frac{1}{r}\,T_d \\ \frac{1}{6\,r^2}\,S_d \end{bmatrix} \tag{11}$$

and finally used as the reference command signals for the sliding mode force control strategy implemented on each muscle (Fig. 2).

Note that the desired torque and stiffness profiles need to be defined on the basis of the mechanical capabilities of the antagonistic joint. Figure 1(a) and 1(b) show the theoretical range of the torque ($T_i = F_i r$) and stiffness ($S_i = k_i r^2$) that each pneumatic muscle can apply at the joint as function of the joint angle and the actual pressure in the muscles.

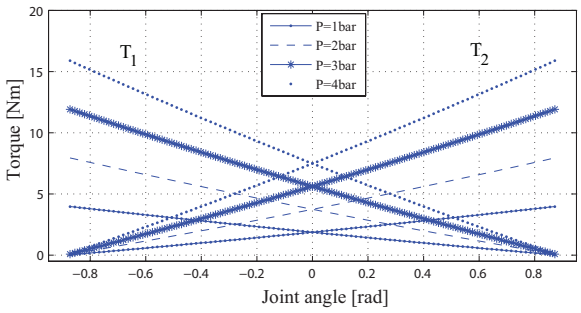


(a)

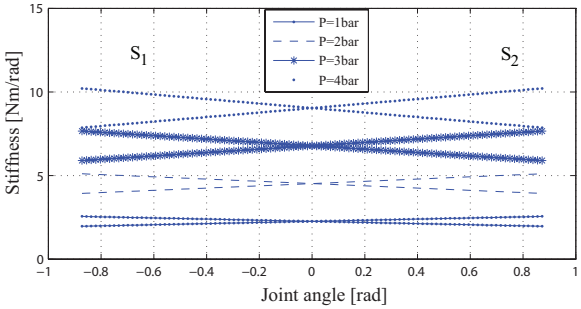


(b)

Fig. 1. Theoretical range of torque (a) and stiffness (b) each pneumatic muscle can apply at the joint as a function of the joint angle and pressure.

### A. Force Controller Design

The first step in designing the force controller for the pneumatic muscle was to convert the discrete valued control input $d_1$ and $d_2$ in (4) into the corresponding duty cycle values $d_{1\%}, d_{2\%} \in [0, 1]$, in order to control the on-off valves through a continuous command signal. An average model of the controlled system (4) was then obtained, that represents a good approximation of the real system for finite but relatively large sampling frequencies [22]

$$\dot{P} = \frac{-P}{\tau} + \frac{P_s}{\tau} u \tag{12}$$

where $u \in [0,\ 1]$ was the control signal. A mapping between the control variable $u$ and the duty cycle $d_{1\%}, d_{2\%}$ was defined as:

$$d_{1\%}, d_{2\%} = \begin{cases} d_{1\%} = u, & d_{2\%} = 0 & \text{if } P < u\,P_s \\ d_{1\%} = 0, & d_{2\%} = 0 & \text{if } P = u\,P_s \\ d_{1\%} = 0, & d_{2\%} = 1 - u & \text{if } P > u\,P_s \end{cases} \tag{13}$$

in order to convert the control signal $u$ into a duty cycle signal for each valve. It is important to highlight that the mapping is not unique and suitable alternative maps between $d_{1\%}, d_{2\%}$ and $u$ can be defined.

Next, the Sliding Mode force Control strategy (SMC) was implemented on each pneumatic muscle. This control strategy was selected for this application since it represents an effective and robust technique for controlling nonlinear systems affected by modeling inaccuracies and parametric uncertainties such as the pMA [23].

To design the SMC controller a sliding surface was considered such as

$$s = P_d - P + \int_{t_0}^{t} (F_d - F)\, d\tau \tag{14}$$

where $P_d$ and $F_d$ represent the desired pressure and force values, respectively. Furthermore, in order to ensure the stability of the system, the SMC control signal $u$ was obtained to satisfy the condition

$$\dot{V} = s\dot{s} < 0 \tag{15}$$

with

$$\dot{s} = \dot{P}_d + \frac{P}{\tau} - \frac{Ps}{\tau} u + F_d - \phi(L)\, P. \tag{16}$$

given by the differentiation of (14), also considering (12) and (1). For this purpose, a continuous equivalent control signal $\hat{u}$ was first formulated solving the dynamics of the sliding mode ($\dot{s} = 0$) such as

$$\hat{u} = \frac{\tau}{P_s} \left[ \left( \frac{1}{\tau} - \phi(L) \right) P + F_d \right] \tag{17}$$

with

$$\phi(L) = \frac{3L^2 - b^2}{4\pi n^2}. \tag{18}$$

Then, to satisfy the condition in (15) in spite of the model uncertainties, an additional switching term was introduced for giving robustness to the control law. The control signal $u$ was therefore obtained such as

$$u = \hat{u} + \lambda \tanh(Ys). \tag{19}$$

Note that the function $\tanh$, instead of the traditional sign function, is introduced for reducing the valve control signal chattering in case of limited tracking error, and the parameter $Y > 0$ is used as smoothing factor. It is noteworthy that by replacing (19) in (16) the stability condition in (15) is verified if $\lambda > \dot{P}_d$, which in turn requires $P_d$ to be continuously differentiable. The complete block scheme of the pneumatic muscle force controller is shown in Fig. 2.

It is important to underline that key factor for the success of the control strategy is the ability of the valves to track relatively high frequency PWM signals [24]. Tracking performance is usually restricted by the significant time delay of the solenoid valves due to both the electro-mechanical time constant and the solenoid driver board implementations. To address this problem, a new speed-up driver circuit was developed to decrease the opening and closing time of the valves allowing for better performance.

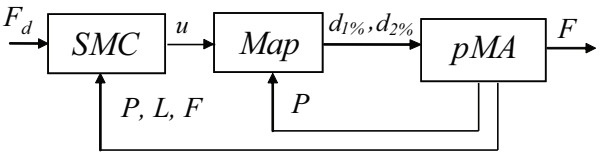


Fig. 2. Block scheme of force controller.

## IV. Experimental Activity

An experimental setup was developed to evaluate the performance of the control strategy (Fig. 3). It consists of a pair of pneumatic muscles antagonistically connected through a pulley of radius 0.024 [m], equipped with an incremental encoder (Avago, series 3300). The length of each pneumatic muscle at rest is 0.17 [m] with an inner diameter of 0.027 [m] (Fig. 3). An inner cylindrical plastic filler, with a length of 0.115 [m] and a diameter of 0.02 [m], is inserted inside the muscle to reduce its dead volume more than 60%. The pneumatic muscle is equipped with a pressure sensor (Honeywell) and a load cell (Burster, model 8417, 1000 [N]) for measuring the inner pressure and the force exerted. The pneumatic muscles are supplied with dry air at 4 [bar] through solenoid valves (Matrix, series 821-2/2 NC) mounted on the joint structure. The supply pipe from the source to the valves is a 6 [mm] inner diameter PVC pipe of length 1.5 [m] while the pipes from the valve to the muscle are 0.15 [m] in length.

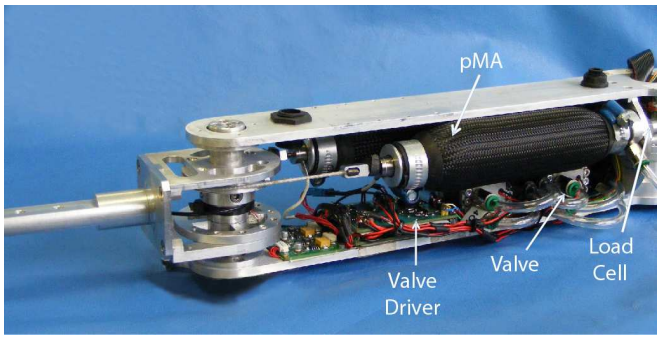


Fig. 3. Experimental setup: 1 DOF joint driven by a pair of pneumatic muscles in antagonistic configuration.

### A. System identification of pneumatic system

The first experiments aimed to identify and validate the simplified model of the valve-pneumatic muscle system introduced in (1) and (12), for static operating condition. A PWM signal with a frequency of 400 [Hz] was generated through software and executed on a PC-104 platform equipped with a Sensorey 526 DAQ board with a 16-bit A/D converter. The results obtained are shown in Fig. 4. During the high state of the PWM signal, a boost current level (1.2 [A]) is supplied by the speed-up driver to the valve, with the aim of pulling the shutter away from the outlet and reducing the valve opening time. This boost current is active for only 0.45 [ms] to prevent valve burnout. Following this a lower current level (0.3 [A] as defined in the valve specification) is supplied to keep the valve open without overdriving it. During the transition to the low state of the PWM, the current flowing through the valve quickly drops to zero and the valve closes (0.2 [ms]).

When an open loop sinusoidal duty cycle was commanded, while measuring the force and pressure, the experimentally estimated bode plot for pressure $G_p(s)$ and force $G_f(s)$ responses were obtained (Fig. 5). Based on the data, the valve-pneumatic muscle system was identified around the working point (P = 3 [bar], L = 0.16 [m]) as a first order system in the frequency range considered ($0.1 - 5$ [Hz]). However, the first order dynamics were affected by a finite time delay as is visible from the phase lag in Fig. 5. This can be ascribed to the tubing, the dead volume of the pneumatic muscle and the valve opening delay time. Moreover, it is possible to observe from Fig. 5 that there were not additional dynamics between the pressure and the force exerted by the pneumatic muscle.

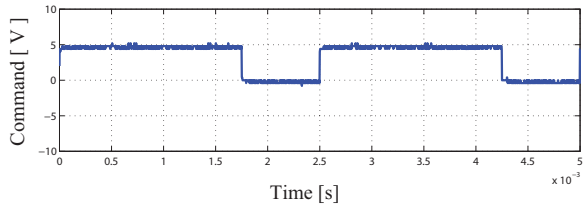


(a) PWM command signal

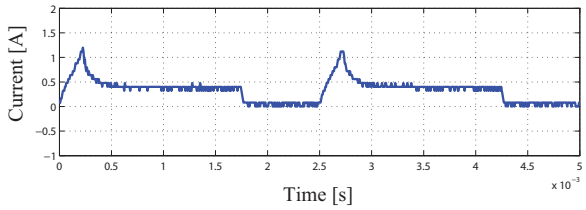


(b) Valve current

Fig. 4. Performance of a solenoid valve driven by PWM command signal at 400 [Hz] with duty cycle 0.7.

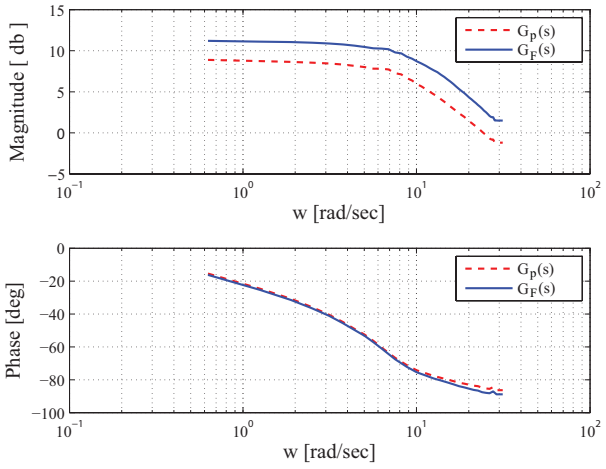


Fig. 5. Experimentally estimated bode plot for pressure and force response. Frequency analysis was conducted for the pneumatic muscle when sending as input to the valves sinusoidal duty ratio in the range of 0.1-5 [Hz].

### B. Control strategy

Suitable experiments were conducted to test the performance of the controlled joint, free to move. The controller frequency was set at 1 [kHz] while the solenoid valves were

driven with PWM signal at 400 [Hz]. The model and control parameters are listed in Table I. Preliminary experiments were carried out to test the force controller in the tracking of sinusoidal waveforms as reference commands $F_d$, while the force $F$, exerted by the pneumatic muscle, was measured through the installed load cell. Figure 6(a) shows the performance of the force tracking for a sinusoidal reference signal with amplitude of 50 [N] and offset of 440 [N] at the frequency of 1.5 [Hz]. This is compared with the resulting force, $F_{sim}$, obtained in simulation for the same reference input. The simulated force controlled pneumatic muscle exhibited comparable performance with the one obtained through experiments, as it can be seen in Fig. 6(b), where the error in force tracking between simulation and experimental data is shown. The implemented force controller was able to track the reference input as expected, and Fig. 6(c) and 6(d) show the commanded duty cycle of the pressurizing and depressurizing valves, respectively.

The joint torque and stiffness control was then tested by checking the controller's ability to track a sinusoidal set point references for the torque, while, simultaneously, the stiffness at the joint followed a sinewave at the same frequency. Figure 7(a) and 7(b) show the performance of the antagonistic actuated joint in tracking a torque signal $T_d$ of amplitude 1 [Nm], offset 6.8 [Nm] at frequency 1.5 [Hz], while the stiffness, $S_d$, was tracking a sinusoidal reference at the same frequency with amplitude of 0.5 [Nm/rad] and offset 5 [Nm/rad]. Also in this case, the results of torque and stiffness control are compared with those obtained in simulation ($T_{sim}$, $S_{sim}$); note that the torque $T$ and the stiffness $S$ at the joint were calculated through (5) and (6), respectively. The tracking error for both torque and stiffness can be seen in Fig. 7(c) and 7(d), respectively. According with the data obtained, the joint controller was able to simultaneously track the set-point references of torque and stiffness, while the joint was free to move. The tracking error was mostly due to the frequency of the PWM signal controlling the valves, in this case 400 [Hz], which ultimately bounded the performance of the controller. With the speed-up driver it is possible to increase the frequency of the PWM, however this drastically reduces the life cycles of the valve.

TABLE I

MODEL AND CONTROL PARAMETERS

| Parameter | Value | Unit |
|---|---|---|
| Ps | 400 | kPa |
| n | 1.4 | |
| b | 0.24 | m |
| $\lambda$ | 0.1 | |
| $\tau$ | 0.1 | s |
| r | 0.024 | m |
| Y | 0.01 | |

## V. CONCLUSION

This paper presented the preliminary results of a torque and stiffness controller for an antagonistically actuated joint with pneumatic muscle actuators. Given the joint torque and stiffness profiles, the forces needed at each pMA were obtained through modeling and then controlled with a sliding mode control technique applied to an average model of the valve-pneumatic muscle system. The experimental results demonstrated the ability of the controller to track sinusoidal torque references while adjusting the joint stiffness. The performance obtained were comparable with the one given

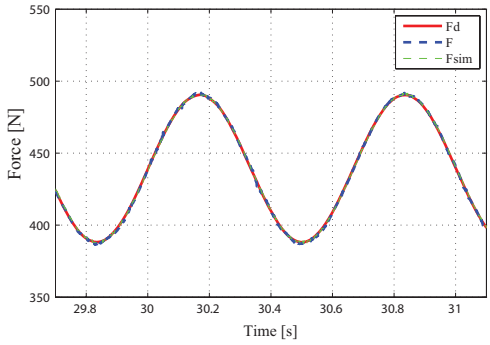


(a) Force tracking

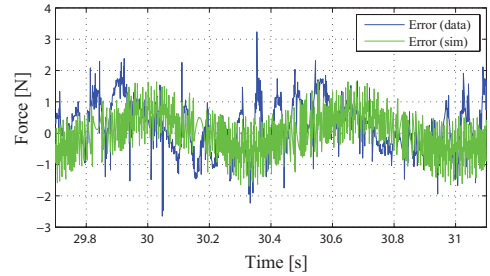


(b) Force error

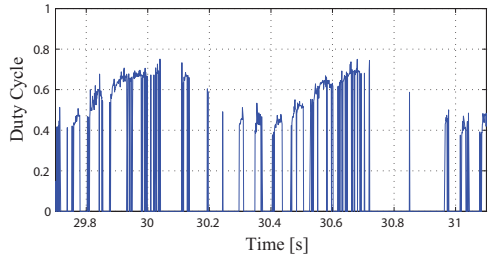


(c) Duty cycle - $d_{1\%}$

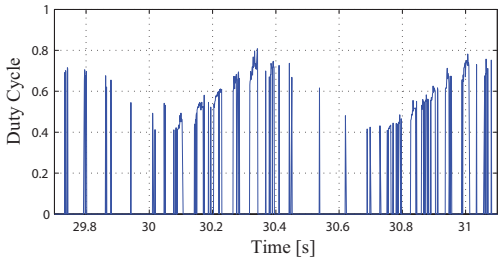


(d) Duty cycle - $d_{2\%}$

Fig. 6. Experimental results of the force controlled pneumatic muscle while tracking sinusoidal set point references at 1.5 [Hz].

by the simulation of the controlled system, identified through frequency analysis. The smooth tracking and the bounded error showed the effectiveness of the control strategy to cope with the uncertainties of the actuation model and the discontinuities of the on/off solenoid valve. The analysis of suitable stiffness profiles for optimizing the performance of the actuation system on the basis of the task requirements will be considered in the future.

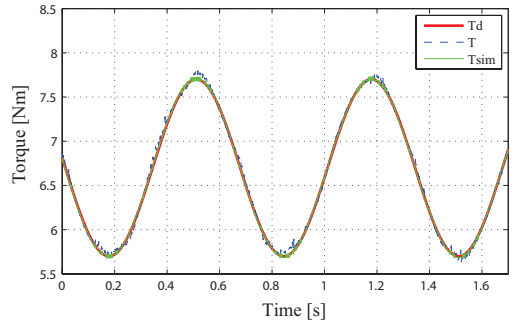


(a) Torque tracking

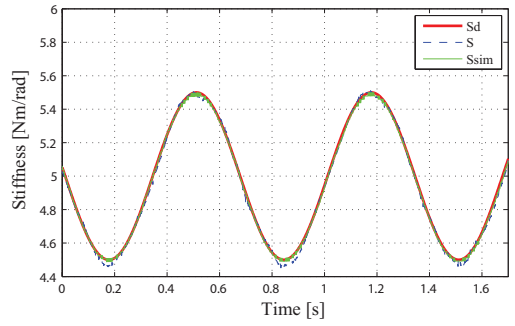


(b) Stiffness tracking

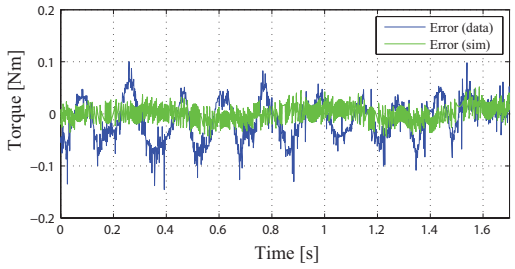


(c) Torque error

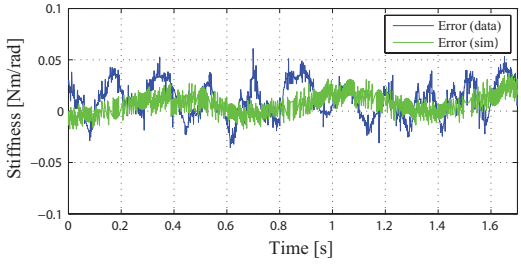


(d) Stiffness error

Fig. 7. Experimental results of the torque and stiffness controlled joint in while tracking sinusoidal set point references at 1.5 [Hz].

## VI. Acknowledgment

This work is supported by VIACTORS, FP7-ICT-2007-3 European STREP project and by the EC Seventh Framework Programme (FP7) under grant agreement no. 216239 as part of the IP DEXMART.

## References

[1] A. De Luca, Haddadin S. Albu-Schäffer, A., and G. Hirzinger. Collision detection and safe reaction with the dlr-*iii* lightweight manipulator arm. *Int. Conf. on Int. Rob. and Sys.*, 2006.

[2] G. Hirzinger, A. Albu-Schaffer, M. Hahnle, and A. Pascucci. Dlr's torque-controlled light weight robot iii - are we reaching the technological limit now? *Int. Conf. on Rob. and Aut.*, 2002.

[3] R. Schiavi, G. Grioli, S. Sen, and A. Bicchi. Vsaii: A novel prototype of variable stiffness actuator for safe and performing robots interacting with humans. *Int. Conf. on Rob. and Aut.*, 2008.

[4] A. Bicchi and G. Tonietti. Fast and soft arm tactics: Dealing with the safety- performance tradeoff in robots arm design and control. *IEEE Robotics and Automation Magazine*, 11(2), 2004.

[5] K. Koganezawa, T. Nakazawa, and T. Inaba. Antagonistic control of multi dof joint by using the actuator with nonlinear elasticity. *IEEE International Conference on Robotics and Automation*, 2006.

[6] S.A. Migliore, Brown E.A., and DeWeerth S.P. Biologically inspired joint stiffness control. *Int. Conf. on Rob. and Aut.*, 2005.

[7] S. Wolf and G. Hirzinger. A new variable stiffness design: matching requirements of the next robot generation. *IEEE International Conference on Robotics and Automation*, pages 1741–1746, 2008.

[8] D. Shin, I. Sardellitti, and O. Khatib. A hybrid actuation approach for human-friendly robot design. *Int. Conf. on Rob. and Aut.*, 2008.

[9] M. Van Damme, B. Vanderborght, B. Verrelst, F. Daerden, and D. Lefeber. Proxy-based sliding mode control of a planar pneumatic manipulator. *Int. Jour. of Rob. Res.*, 2008.

[10] S. Davis and D.G. Caldwell. Braid effects on contractile range and friction modeling in pneumatic muscle actuators. *IJRR*, 2006.

[11] P. C. Chou and B. Hannaford. Measurement and modeling of mckibben pneumatic artificial muscles. *Trans. Rob. Autom*, 1996.

[12] Klute G. K. and Hannaford B. Fatigue characteristics of mckibben artificial muscle actuators. pages 1776–1781, 1998.

[13] A. Bicchi, L. S. Rizzini, and G. Tonietti. Compliant design for intrinsic safety: general issues and preliminary design. *IROS*, 2001.

[14] G. Tonietti and A. Bicchi. Adaptive simultaneous position and stiffness control for a soft robot arm. *Int. Conf. on Int. Rob. and Sys.*, 2002.

[15] B. Vanderborght, B. Verrelst, R. Van Ham, M. Van Damme, D. Lefeber, B. M. Y. Duran, and P. Beyl. Exploiting natural dynamics to reduce energy consumption by controlling the compliance of soft actuators. *Int. J. Rob. Res.*, 2006.

[16] D.W. Repperger, K.R. Johnson, and C. A. Phillips. Nonlinear feedback controller design of a pneumatic muscle actuator system. *American Control Conference*, 1999.

[17] E. Barth, J. Zhang, and Goldfarb M. Sliding mode approach to pwm controlled pneumatic system. *Amer. Contr. Conf.*, 2002.

[18] R. B. Van Varseveld and G. M. Bone. Accurate position control of a pneumatic actuator using on/off solenoid valves. *Trans. on Mech.*, pages 195–204, 1997.

[19] W. Colbrunn, G. M. Nelson, and D. R. Quinn. Modeling of braided pneumatic. actuators for robotic control. *IROS*, 2001.

[20] K. Inoue. Robberactuators and applications for robots. *Int. Sym. of Rob. Res.*, 1987.

[21] H.S. Ramirez, P. Lopez, and B. Tondu. On the robust stabilization and tracking for robotic manipulators with artificial muscles. *Int. Jour. of Sys. Science*, 1996.

[22] H. S. Ramirez. A geometric approach to pulse width modulated control in nonlinear dynamical systems. *Trans. on Aut. Contr.*, 1989.

[23] J. J. E. Slotine. Applied nonlinear control. 1991.

[24] V.I. Utkin. Variable structure control system with sliding mode. *Trans. Aut. Contr.*, pages 222–230, 1977.